Impedance estimator for multi-source DC microgrids with islanding detection capabilities

Cristian Blanco, Pablo Garcia, Andres Suarez and Irene Pelaez
LEMUR Research Group
University of Oviedo
Gijon, Spain
Email: blancocristian@uniovi.es, garciafpablo@uniovi.es, suarezandres@uniovi.es, pelaezirene@uniovi.es
www.lemuruniovi.com

***Abstract*—DC microgrids with integrated distributed generators (DGs) require island detection in all converters. This work proposes an impedance estimation strategy to detect the grid connection status among all active participants in the DC microgrid. The method is based on a pulse signal injection (PSI) combined with the recursive least squares (RLS) algorithm to estimate the equivalent parallel resistance and capacitance of the components connected to the DC bus (both active and passive). This technique allows to detect islanding conditions by using the estimated capacitance value as a reliable metric. Compared with the existing DC island detection technology, this method: 1) does not have a non-detection region; 2) has a little impact on the DC bus voltage; 3) provides simultaneous islanding detection for all converters of the DC microgrid and 4) avoids using a dedicated communication layer. The method is verified in single and multi-converter scenarios.**

***Index Terms*—current control, DC-DC converters, DC microgrids, impedance estimation, islanding detection**

I. Introduction

Over the past few years, microgrids, energy storage systems, distributed power generation techniques, electric vehicles, and LED lighting have been the focus of significant efforts to develop low-carbon-footprint technologies. Although AC microgrids were first developed, DC and AC/DC hybrid microgrids have become popular in the past decade [1], [2].

In a typical AC/DC hybrid microgrid, the distributed power generation units share the DC bus with energy storage systems, electric vehicle charging stations, public lighting, telecommunications equipment, and inverters for some household or industrial applications. At the same time, AC-DC converters are used as interfaces for AC networks, and they are usually responsible for controlling the DC bus voltage. In this case, it is essential to know the connection status to the converter that forms the DC microgrid to achieve a fast and seamless transition to the DC bus voltage control in the event of a fault [3]. This technique is called island detection, and some methods for performing this detection have previously been proposed for DC microgrids [4]–[12].

The working principle of the islanding detection techniques for DC microgrids is based on the observation of bus voltage changes through a monitoring system (passive implementation [6]) or a forced feedback system (active implementation [7], [9], [13]). While the first group shows some non-detection regions (mainly when the amount of power generated is around consumption), the second group can cause a sudden change in the grid voltage amplitude [5], [7], which reduces the quality of service.

This paper proposes an impedance estimation technique with islanding detection capabilities. The proposed technique uses the RLS algorithm to estimate the DC bus impedance based on the parallel Resistance-Capacitance (RC) modelling. A PSI technique [14] is used to ensure the accuracy of RLS. The method is suitable for single-converter and multi-converter solutions and allows fast, accurate, and simultaneous estimation of grid connection status. At the same time, it does not require any dedicated communication layer, and its performance is independent of the microgrid topology. It is finally noted that the bus voltage is slightly affected, improving the preceding islanding detection techniques for DC microgrids.

The paper is organized as follows: Section 2 carries out the theoretical analysis, including the system modeling, PSI injection solutions, and the RLS algorithm implementation. Section 3 provides the method evaluation in single and multi-converter scenarios, while Section 4 gives the conclusions of the work.

II. Theoretical Analysis

Fig. 1 shows the topology of the DC microgrid that will be used through this work. It is composed by a parallel connection of a pair of DC-DC converters, a resistance (R) that emulates the load demand and a DC grid (v_g) connected to the bus through a breaker (B). The grid model includes a series resistance (R_g) that models a finite-power connection and the capacitance of the AC/DC grid converter (C_g).

One of the converters, called *Leader* in this work, will be in charge of controlling the DC bus in island mode. Thus, it will behave as a voltage source in island mode (IM) and as a current source in grid-connected mode (GCM). The other converter (called *Follower*) works as a grid feeding converter so it behaves as a current source in both states. Other control strategies may be used (like droop control [15]), but this issue does not impact the proposed impedance estimation technique.

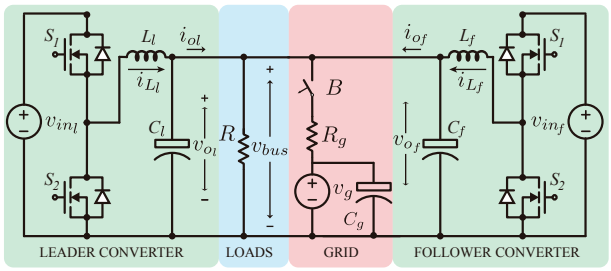

Fig. 1: Topology of the DC microgrid under study.

A. System Modeling

Fig. 2 shows the DC-bus model that will be used as a reference. It is mainly composed by a parallel connection of a resistance (R) and a capacitance (C). Thus, the equivalent impedance of the elements connected to the DC bus follows (1).

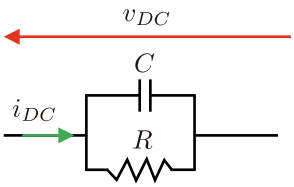

Fig. 2: Parallel RC Model.

$$Z_{eq}(s) = \frac{v_{DC}(s)}{i_{DC}(s)} = \frac{R}{RCs+1} \tag{1}$$

The key point here is to obtain the equivalent RC impedance under single and multi-converter scenarios, both in IM and GCM. According to the system description in Figs. 1 and 2, and for the particular case of a single-converter operation, the output impedance of the converter (after the LC filter) may be modeled in GCM as an RC parallel circuit (1), being R in this case the load demand and C the grid capacitance (C_g, see Fig. 1). Conversely, in IM, the output impedance of the converter follows a simple resistive circuit, defined by the equivalent load demand (R), being C zero in this case.

TABLE I: Setup Parameters

Symbol	Parameter	Value
v_{in_l}, v_{in_f}	Input voltage	70 V
v_{bus},v_g	DC bus voltage	48 V
R	Load bus (2.5 kW)	0.9 Ω
f_s, f_{RLS}	Switc. & RLS freq.	10 kHz
L_l	Leader inductance	2 mH
L_f	Follower inductance	2.2 mH
C_l, C_f	Lead. & Foll. cap.	270 μF
C_g	Grid capacitance	2700 μF
R_g	Grid resistance	0.2 Ω
BW_I	Current control BW	500 Hz
ω_{PSI}	Pulse frequency	1000 Hz
v^*_{PSI}	Pulse magnitude	0.05 p.u.
W_{PSI}	Pulse width	.25 p.u.

When more than one converter are connected in parallel, the converter output impedance varies from the single-converter scenario. In this case, each converter can be modeled as a variable resistance (2), whose value depends on the bus voltage (v_{bus}) and the converter injected/absorbed power ($P_{l,f}$) [16]. Note that a passive sign convention is used in this work, meaning that a positive resistance means that the converter is absorbing power while a negative impedance means that the converter is injecting power to the bus.

$$R_{l,f} = \frac{v_{bus}^2}{P_{l,f}} \tag{2}$$

Therefore, the RC parallel modelling (1) can be also be used both in IM and in GCM for multi-converter scenarios, the output impedance of each converter following (2). In IM, the equivalent resistance results from the parallel connection of the load demand (R) and the resistance of the other converters connected to the DC bus (2). At the same time, the estimated capacitance results from the equivalent capacitance of the other converters connected to the DC bus.

It is finally noted that when the microgrid is in GCM, the estimated resistance does not vary from the IM case. In this case, the estimated capacitance results from the parallel connection between the grid capacitance (C_g) and the capacitance of the other converters connected to the bus ($C_{f,l}$).

B. Islanding detection in DC microgrids.

It has been proven that a parallel RC modeling accurately fits the converter output impedance. It has also been shown that the equivalent capacitance of this model can be used for islanding purposes since it has a noticeable variation from IM to GCM, both in single and in multiple-converter scenarios. Thus, the proposed islanding detection technique is based on the converter output impedance estimation.

This will be done by using the RLS algorithm for the parameter identification of system (1). The converter will add a pulse train excitation voltage to its duty cycle to estimate its output impedance. The PSI injection has been selected in this work since it does not require any modification in the converter control structure. Note that other types of excitation may be used, e.g. sinusoidal, the behavior of the proposed technique being independent of the excitation technique.

1) PSI and parameter selection: Two PSI methods may be used: voltage or current-based, their implementations being shown in Fig. 3. In the voltage-based injection technique, Fig. 3a, the PSI is added as a duty-cycle perturbation to the proportional-integral (PI) controller command (v^*_{PSI} in Fig. 3a). On the other hand, the current-based injection implementation (Fig. 3b) adds the PSI as a reference to the current control loop (i^*_{PSI} in Fig. 3b). Depending on the pulse train frequency this requires to have high-bandwidth current controllers so the PSI voltage injection has been used in this work. A pulsed disturbance of 1kHz, 0.05 p.u.magnitude and 25% duty cycle will be used.

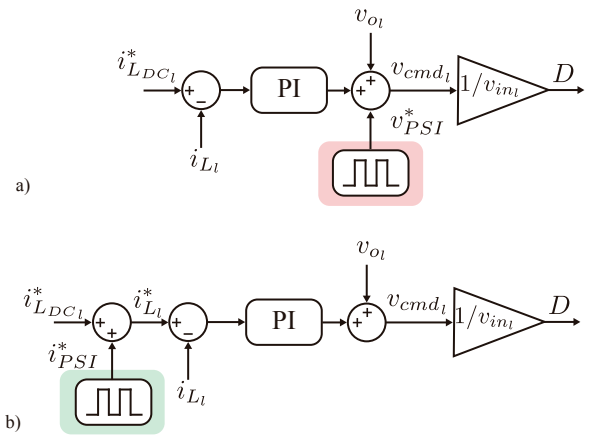

Fig. 3: a)Voltage and b)current PSI techniques.

2) RLS Algorithm Implementation: The proposed technique is based on the RLS method for system identification [17]. The RLS algorithm works as an adaptive filter and allows to obtain an online estimation of the equivalent RC model (1) ($\hat{R}, \hat{C}$) from the measured converter output voltage (v_{olf}) and current (i_{olf}). In each RLS iteration, the estimation error ($e(n)$ in Fig. 4) is minimized by updating the filter coefficients online. This technique has previously used for for grid impedance estimation in three-phase systems [14] and DC-Bus health estimation in back-to-back converters with doubly-fed induction generators [18]. Benefits of the RLS algorithm include low data storage and reduced computational effort.

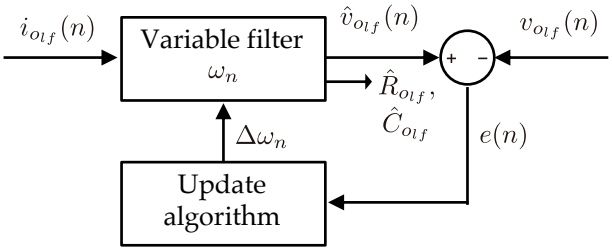

Fig. 4: RLS Algorithm Implementation.

Since the RLS works in the discrete domain [17], the bilinear transform (3) has been used to obtain the converter output impedance transfer function in the discrete domain (4), being T the selected sampling period. At the same tine, Algorithm 1 contains the implementation of the RLS algorithm for the current application. In this case, λ sets the forgetting factor (usually $0.9 < \lambda < 1$, $\lambda = 0.995$ in this case). In each iteration the ω_n array will contain an estimation of the filter coefficients of the discrete transfer function (4), where the actual and the last samples of the capacitor voltage and current are inputs to the RLS algorithm. Thus, the output impedance estimated parameters ($\hat{R}, \hat{C}$) can be calculated by using (4), (5) and (6) as (7).

$$s = \frac{2}{T}\frac{z-1}{z+1} \tag{3}$$

$$Z_{RC}(z) = \frac{0.5RT\ (z+1)}{CRz + 0.5\ T\ z - CR + 0.5\ T} \tag{4}$$

$$v_{DC}[n] = \frac{b_0[i_{DC}[n] + i_{DC}[n-1]] - a_1\, v_{DC}[n-1]}{a_0} \tag{5}$$

$$\omega_n = \frac{1}{\hat{a_0}} \cdot [\hat{b_0}, \hat{a_1}] \tag{6}$$

$$\hat{R} = \frac{-2\omega_n[1]}{\omega_n[2] - 1}, \quad \hat{C} = \frac{T\,(\omega_n[2] + 1)}{4\omega_n[1]} \tag{7}$$

Algorithm 1 RLS algorithm.

$\omega_n = zeros(1, 2)$
$P_n = identity(2) \cdot 10^{10}$
$g_n = zeros(2, 1)$;
$\alpha_n = 0$
while true **do**
  $X_n = [i_{o_{l,f_n}} + i_{o_{l,f_{n-1}}}, v_{o_{l,f_{n-1}}}]$
  $\alpha_n = v_{o_{l,f_n}} - X'_n \cdot \omega'_n$
  $g_n = \frac{P_n \cdot X_n}{\lambda + X'_n \cdot P_n \cdot X_n}$
  $P_n = \frac{1}{\lambda} \cdot \frac{P_n - (P_n \cdot (X_n \cdot X'_n) \cdot P_n}{\lambda + X'_n \cdot P_n \cdot X_n}$
  $\Delta\omega = (\alpha_n g_n)'$
  $\omega_n = \omega_n + \Delta\omega$
end while

III. Simulation Evaluation

The evaluation of the proposed method has been performed by means of simulations in MATLAB/Simulink. In order to test the performance of the proposed method, the setup shown in Fig. 1 was used. The Setup parameters are shown in Table I.

A. Single-converter operation

Fig. 5 shows the simulation results for the single-converter operation (Fig. 1). Fig. 5a shows the breaker B connection status and the breaker command for a second load connection.

The *Leader* converter starts isolated from the grid, feeding a local load of $2.5kW$, and a grid connection is performed at t=0.5s. The converter is returned to IM at t=1.5s. A load step ($2.5\ kW$) is performed at t=0.25s, where an additional $R = 0.9\Omega$ is connected to the DC bus, the load being disconnected at t=1.25s.

Fig. 5b shows the converter output current (i_{ol} in Fig. 1). The converter injects the necessary amount of current to maintain the DC bus voltage to 48V, including at the same time the PSI that leads to a small perturbation (0.2V, $\approx$ 0.004 p.u.) in the DC bus voltage in IM (Fig. 5c). At the same time, Fig. 5d shows the RLS coefficients (6). Note the noticeable changes when grid connection events occur ($t = 0.5s, t = 1.5s$).

The estimated output resistance ($\hat{R}_{o_l}$) of the parallel RC model (1) is shown in Fig. 5e. The load connected to the DC

bus is accurately estimated, both in IM and in GCM for the different load conditions (0.9 or 0.45 Ω).

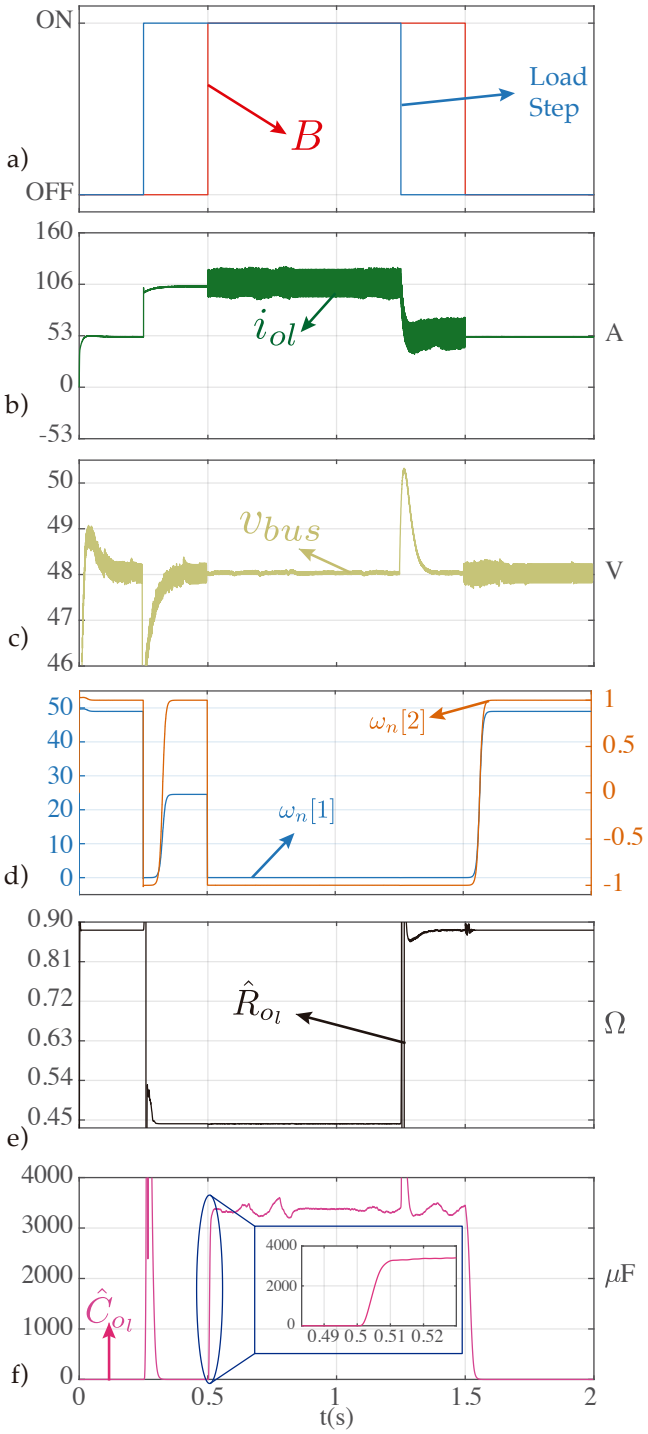

Fig. 5: Simulation evaluation for single scenario: a) breaker status, b) converter output current ($i_{o_{lf}}$), c) bus voltage (v_{bus}), d) RLS coefficients of the *Leader* Converter (Fig. 4) and estimated converter output e) resistance ($\hat{R}_{o_l}$) and f) capacitance ($\hat{C}_{o_l}$).

The estimated output capacitance ($\hat{C}_{o_l}$) is shown in Fig. 5f. Note that this value rounds 0 in IM (there is not another capacitor connected to the bus than the converter one) and it is higher than 3000 μF in GCM. Note that a transient in the estimated capacitance occurs when the second load is connected/disconnected to the bus (t=0.25s and t=1.25s). However, this does not affect to the accuracy of the proposed technique since both estimations are affected at the same time ($\hat{R}_{o_l}$ and $\hat{C}_{o_l}$) while only the estimated capacitance is affected when the grid is connected/disconnected. Thus, the proposed technique shows an excellent response detecting the islanding situation (detection takes less than 10 ms.).

B. Multi-converter operation

Results for the multi-converter scenario are shown in Fig. 6, where the same test procedure as in the single-converter scenario was performed. In this case, the *Leader* and *Follower* converters are controlled to inject both positive and negative currents as shown in Fig. 6b. At the same time, the PSI was injected from the two converters at different points in time. The *Leader* injects them in $t < 1s$, while the *Follower* injects them in $1 < t < 2s$. Variations in the converter injected currents have impact in the bus voltage (Fig. 5c), although the nominal voltage is recovered after some transients.

The RLS coefficients are shown in Fig. 6d and Fig 6e for the *Leader* and *Follower* converters respectively. Note that the variations in the output resistance are mainly correlated with load or converter power variations ($t = 0.25s, t = 0.4s$ etc..) and with the $\omega_n[2]$ coefficient, while changes in the grid connection status ($t = 0.5s, t = 1.5s$) are mainly correlated with the $\omega_n[1]$ coefficient.

The estimated output resistances of the *Leader* and *Follower* converters ($\hat{R}_{olf}$) are shown in Fig. 5f, and they match those obtained in the theoretical analysis since they depend on the converter injected or absorbed power (2). It is finally shown in Fig. 6g the *Leader* and *Follower* estimated capacitance values($\hat{C}_{lf}$). In IM both estimate the capacitance of the other converter ($\approx$ 270 μF) and in GCM both estimate a high capacitance value, having enough distance from the capacitance in island mode to rely on the estimation. It must be noted that both converters are able to detect the islanding situation in approximately 10 ms.

IV. Conclusion

This paper proposed an impedance detection technique with islanding detection capabilities. The method is valid for single and multi-source DC microgrids and it based on the discrete-time system modeling, a PSI and the RLS technique. A theoretical analysis was performed, while the control and parameter selection guidelines were also developed. The proposed method allows simultaneous islanding detection of all converters connected to the DC bus by looking to the estimated resistance and capacitance values. The method was validated by a theoretical analysis, as well as by a set of simulation tests. From the obtained results it can be concluded the high reliability, fast detection, and smooth transient response of the method, while its accuracy is independent from the microgrid topology.

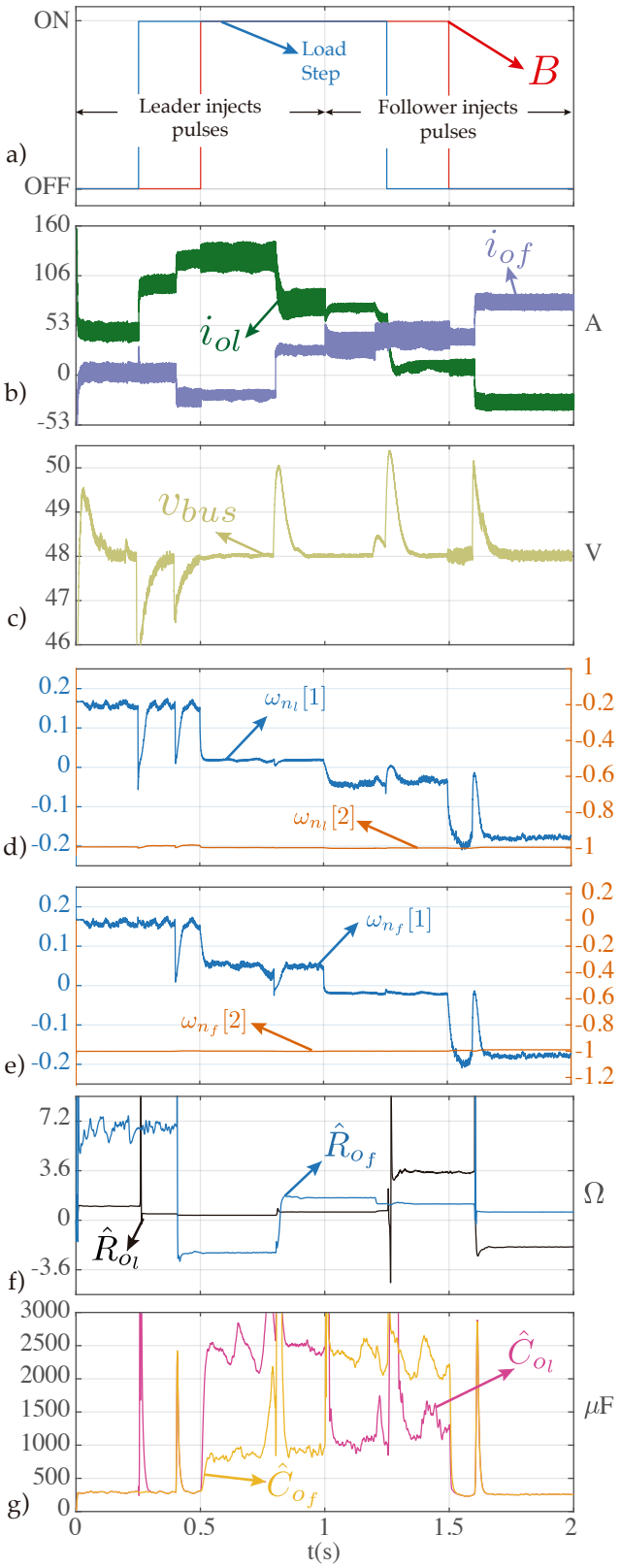

Fig. 6: Simulation evaluation for multi-converter scenario: a) breaker status, b) converter output current ($i_{o_{lf}}$), c) bus voltage (v_{bus}), RLS coefficients of the d)*Leader* and e) *Follower* Converters (Fig. 4). Estimated converter output d) resistance ($\hat{R}_{o_{lf}}$) and e) capacitance ($\hat{C}_{o_{lf}}$).

References

[1] P. Yang, Y. Xia, M. Yu, W. Wei, and Y. Peng, "A decentralized coordination control method for parallel bidirectional power converters in a hybrid ac dc microgrid," *IEEE Trans. on Ind. Elec.*, vol. 65, no. 8, pp. 6217–6228, Aug 2018.

[2] A. Navarro-Rodriguez, P. Garcia, R. Georgious, and J. Garcia, "Adaptive active power sharing techniques for dc and ac voltage control in a hybrid dc/ac microgrid," *IEEE Trans. on Ind. App.*, vol. 55, no. 2, pp. 1106–1116, March 2019.

[3] L. Meng, Q. Shafiee, G. F. Trecate, H. Karimi, D. Fulwani, X. Lu, and J. M. Guerrero, "Review on control of dc microgrids and multiple microgrid clusters," *IEEE Journal of Emerging and Selected Topics in Pow. Elec.*, vol. 5, no. 3, pp. 928–948, Sep. 2017.

[4] F. Paz and M. Ordonez, "An impedance-based islanding detection method for dc grids," in *2018 9th IEEE International Symposium on Pow. Elec. for Distributed Generation Systems (PEDG)*, June 2018, pp. 1–7.

[5] A. M. I. Mohamad and Y. A. I. Mohamed, "Impedance-based analysis and stabilization of active dc distribution systems with positive feedback islanding detection schemes," *IEEE Trans. on Pow. Elec.*, vol. 33, no. 11, pp. 9902–9922, Nov 2018.

[6] G. Seo, K. Lee, and B. Cho, "A new dc anti-islanding technique of electrolytic capacitor-less photovoltaic interface in dc distribution systems," *IEEE Trans. on Pow. Elec.*, vol. 28, no. 4, pp. 1632–1641, April 2013.

[7] A. M. I. Mohamad and Y. A. I. Mohamed, "Assessment and performance comparison of positive feedback islanding detection methods in dc distribution systems," *IEEE Trans. on Pow. Elec.*, vol. 32, no. 8, pp. 6577–6594, Aug 2017.

[8] C. N. Papadimitriou, V. A. Kleftakis, and N. D. Hatziargyriou, "A novel method for islanding detection in dc networks," *IEEE Trans. on Sust. Energy*, vol. 8, no. 1, pp. 441–448, Jan 2017.

[9] S. Dhar and P. K. Dash, "Performance analysis of a new fast negative sequence power injection oriented islanding detection technique for photovoltaic photovoltaic based voltage source converter based micro grid operation," *IET Gen., Trans. Dist.*, vol. 9, no. 15, pp. 2079–2090, 2015.

[10] W. Song, Y. Chen, A. Wen, Y. Zhang, and C. Wei, "Detection and switching control scheme of unintentional islanding for hand-in-hand dc distribution network," *IET Gen., Trans. Dist.*, vol. 13, no. 8, pp. 1414–1422, 2019.

[11] X. Chen, Y. Li, and P. Crossley, "A novel hybrid islanding detection method for grid-connected microgrids with multiple inverter-based distributed generators based on adaptive reactive power disturbance and passive criteria," *IEEE Trans. on Pow. Elec.*, vol. 34, no. 9, pp. 9342–9356, Sep. 2019.

[12] *Hybrid Islanding Detection for AC/DC Network Using DC-link Voltage*, Aug 2018.

[13] A. M. I. Mohamad and Y. A. I. Mohamed, "Analysis and mitigation of interaction dynamics in active dc distribution systems with positive feedback islanding detection schemes," *IEEE Trans. on Pow. Elec.*, vol. 33, no. 3, pp. 2751–2773, March 2018.

[14] P. Garcia, M. Sumner, A. Navarro-Rodriguez, J. M. Guerrero, and J. Garcia, "Observer-based pulsed signal injection for grid impedance estimation in three-phase systems," *IEEE Trans. on Ind. Elec.*, vol. 65, no. 10, pp. 7888–7899, Oct 2018.

[15] G. Liu, T. Caldognetto, P. Mattavelli, and P. Magnone, "Power-based droop control in dc microgrids enabling seamless disconnection from upstream grids," *IEEE Trans. on Pow. Elec.*, vol. 34, no. 3, pp. 2039–2051, March 2019.

[16] F. Paz and M. Ordonez, "High-accuracy impedance detection to improve transient stability in microgrids," *IEEE Trans. on Ind. Elec.*, vol. 64, no. 10, pp. 8167–8176, Oct 2017.

[17] L. Ljung, *System Identification: Theory for the User*. Upper Saddle River, NJ, USA: Prentice-Hall, Inc., 1986.

[18] C. Blanco, P. García, C. Gómez-Aleixandre, and I. Pel, "Online parameter estimator of the dc bus capacitor bank for doubly-fed induction generators," in *2019 21st European Conference on Power Electronics and Applications (EPE '19 ECCE Europe)*, 2019, pp. P.1–P.9.